Available online at www.sciencedirect.com

ScienceDirect

Procedia CIRP 45 (2016) 187 – 190

www.elsevier.com/locate/procedia

3rd CIRP Conference on Surface Integrity (CIRP CSI)

# Analysis of abrasion mechanisms in the AISI 303 stainless steel: Effect of deformed layer

V. Seriacopi[a]*, N. K. Fukumasu[a], R. M. Souza[a], I. F. Machado[a]

[a]*Surface Phenomena Laboratory, Polytechnic School, University of Sao Paulo, Av. Prof. Mello Moraes, 2231, Sao Paulo, 05508-030, Brazil*

*Corresponding author. Tel.: +551130919868; fax: +551130915461. E-mail address: vanessaseriacopi@usp.br

**Abstract**

Austenitic stainless steel is used in many industrial applications, especially those in which the corrosion resistance is relevant. However, this material is susceptible to surface damage, as well as the occurrence of phase transformations during manufacturing or even throughout use, since they present high work hardening. Therefore, the surface integrity cannot be neglected. This work aims studying the mechanical behavior of AISI 303 stainless steel during scratch tests. Analyses were conducted at the microstructural level, considering the presence of MnS inclusions. Scratch tests with normal loads on the order of mN were carried out using a diamond stylus to simulate the action of a single abrasive particle. The effect of surface finishing was evaluated by testing surfaces with mechanical or electrolytic polishing, which differ in terms of the presence (in the mechanical) or absence (in the electrolytic) of a deformed layer close to the specimen surface. The results allowed estimating the transition loads between abrasion mechanisms, from micro-ploughing to microcutting. These loads were determined for the different surface finishing. Preliminary numerical simulations were also included. In single abrasive operations, numerical results indicated the trend in decreasing the mass removed when the strain-hardened layer is considered.



Peer-review under responsibility of the scientific committee of the 3rd CIRP Conference on Surface Integrity (CIRP CSI)

Keywords: Stainless Steel; Abrasion; Surface Finishing.

## 1. Introduction

The wide industrial application of austenitic stainless steels is mainly justified by their corrosion resistance [1]. The British Stainless Steel Association [2] reported their benefits in medical, pharmaceutical and food processing areas. These materials are non-magnetic and represent 65-70% of the stainless steel grades [2].

Despite the benefits regarding corrosion resistance, these materials are usually susceptible to the surface damage, as well as the occurrence of phase transformations during manufacturing or use, due to high work hardening [3]. Another unfavorable point is the mechanism of built up edge formation during cutting, which often leads to the adhesive wear of tools [4].Thus, the surface integrity can be negatively affected depending on the tribological conditions encountered in the application. Although the stainless steel work hardening is presented as a disadvantage throughout the machining operations, many researches [5–9] have shown the high strain-hardening rate and the deformation-induced transformation as positive aspects regarding the workpiece applications and mechanical properties.

The work conducted by Avery presented a comparison of the tribological behavior of electropolished or abraded stainless steel surfaces, considering the existence of a hardened layer in the last one [10]. Hokkirigawa, Kato and Li [11] characterized the evolution of abrasive mechanisms in austenitic stainless steels, from the mild abrasion or ploughing to the severe abrasion or cutting. In view of this background, this work aims to study the mechanical behavior of AISI 303 stainless steel during scratch tests. Analyses were conducted with loads on the order of mN, such that material behavior is affected by the presence of MnS inclusions. The effect of surface finishing was evaluated by testing surfaces with mechanical and electrolytic polishing. The results allowed estimating the transition loads between abrasion mechanisms, from micro-ploughing to microcutting [11]. These mechanisms were considered to evaluate the effect of a single abrasive on the materials microstructure. In brief, the approach in this work consists in a simplified analysis that



Peer-review under responsibility of the scientific committee of the 3rd CIRP Conference on Surface Integrity (CIRP CSI)

doi:10.1016/j.procir.2016.02.326

correlates with manufacturing operations with non-defined tool geometry, such as grinding. Moreover, preliminary numerical simulations were developed to verify possible differences concerning the experimental mass removal during the scratch tests.

## 2. Materials and Methods

**Materials.** In this work, specimens of AISI 303 and 304 were studied. The nominal chemical composition (%wt) of AISI 303 is 17.20Cr, 8.21Ni, 1.88Mn, 0.48Si, 0.05C, 0.2S and 0.04P. This composition is the result of the addition of sulfur to the composition of AISI 304 stainless steel, which contains only 0.03 %wt of sulfur, in order to obtain MnS inclusions that usually improve the material machinability [5,12]. The longitudinal sections of bars with diameter equal to 25 mm were evaluated (rolling direction). Assuming that the austenitic matrix of both materials is similar, Vickers microhardness tests were conducted only on AISI 304, to get information from the steel matrix, avoiding the effect of the higher volume fractions of MnS. This procedure allows comparison with literature results [10,11]. Furthermore, scratch tests were conducted only on AISI 303 specimens.

**Surface finishing preparation.** The microstructure of AISI 303 steel was observed by scanning electron microscopy (SEM - Jeol JSM 6010-LA) with energy dispersive X-ray spectroscopy (EDS). Specimen preparation consisted of mechanical or electrolytic polishing. Mechanical polishing causes a strain-hardened layer that can be removed by electrolytic polishing. Therefore, two different conditions at the surface and subsurface were obtained.

The mechanical polishing consisted of grinding and polishing down to 0.04 µm colloidal silica suspension. Further electrolytic polishing was carried out in one sample. The electrolyte composition was: 800 mL of ethyl alcohol, 140 mL of distilled water and 60 mL of perchloric acid. The electrolyte was kept below 10 °C and samples were polished at 40 V for 20 s. The area exposed was 1 cm², following the literature recommendations [13].

**Mechanical properties evaluation.** Vickers microhardness tests were conducted on the AISI 304 steel specimen, selecting loads of 50, 100, 500 and 2,000 gf. One-Way analysis of variance was performed to calculate the pre-hardened layer thickness in view of the different depths of penetration [14,15].

**Scratch tests.** Scratch tests were conducted on AISI 303 samples in order to study the action of a single abrasive at the microscale. TI-950 Hysitron triboindenter was applied for these tests. The High Load module was selected and tests were conducted with constant normal forces. The scratch test stylus was a diamond conical indenter with 5 µm tip radius and internal angle of ~ 60°. The scratch procedure consisted of the following steps: (i-) surface profilometry; (ii-) indentation or loading; (ii-) scratching; and (iv-) unloading. The scratch length was 400 µm, with 10 µm.s$^{-1}$ linear velocity. Two repetitions were performed for each normal load.

The range of normal forces applied during the scratches was selected based on the abrasion mechanisms map reported by Hokkirigawa, Kato and Li [11]. Therefore, the range from 5 to 50 mN was estimated to cover all the abrasive mechanisms (see Figure 1). The degree of penetration ($D_p$) in Figure 1 is a parameter that indicates the severity of mass removal and can be determined using Eq. (1) [11], where: R is the tip radius of the abrasive (5 µm); H is the slab hardness (200 HV); and W is the normal force (from 5 to 100 mN).

$$D_p = R\left(\frac{\pi H}{2W}\right)^{1/2} - \left(\frac{\pi R^2 H}{2W} - 1\right)^{1/2} \quad (1)$$

After the scratch tests, AISI 303 steel specimens were characterized by SEM, and by Coherence Correlation Interferometry (CCI-MP Taylor Hobson), which allowed evaluating the 3D topography.

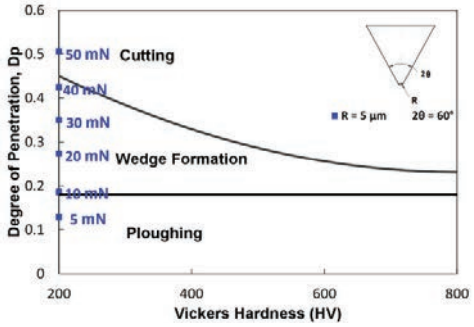


Fig. 1. Abrasion mechanisms estimated for the homogeneous austenitic stainless steel (AISI 304) in view of Hokkirigawa, Kato and Li's work [11].

**Computational Simulation.** A two-dimensional (2D) numerical model of the scratch tests was developed using the Finite Element Method (FEM), in Abaqus/Explicit 6.13® software. Plane stress and constant normal force were considered throughout the scratches. The abrasive particle was modeled with a 5 µm tip radius and with a rigid-analytical surface. Four materials were tested as the slab: the homogeneous case (304 steel - austenitic matrix), with and without the presence of the strain-hardened layer; and the heterogeneous material (303 steel – austenitic matrix with MnS), with and without the effect of that previously calculated strain-hardened layer. It was assumed that the slab phases (matrix and sulfides) were elastic-plastic, with mechanical properties (modulus of elasticity, yield stress and strain-hardening coefficient) obtained by experimental instrumented indentation, using 10 mN load. The densities and Poisson ratio were obtained in the literature [16,17]. The damage parameters for nucleation and propagation were specified according to the literature [18]. In each simulation, the slab was discretized with quadrilateral elements (CPE4R type). The smallest element of the mesh had an edge of 0.5 µm.

## 3. Results

### *3.1. Surface Finishing Characterization*

Figure 2 displays the structure of the longitudinal section of the AISI 303 steel bar, characterized by SEM and EDS. The figure indicates an austenitic matrix and MnS inclusions. In addition, composition maps from EDS analysis show higher levels of Mn and S in the inclusions, denoted by the color scales. Five measurements of the 3D topography were carried out in different areas of the surfaces of each sample. The calculated topography parameters are displayed in Table 1. Values indicate that the electropolished surface is rougher, has a higher density of peaks, and sharper asperities. Bhuyan et al. [19] reported that a more efficient control of the electrolytic polishing parameters, such as electrolyte temperature, current density, polishing time and pulsed current application, is necessary to adjust the flatness and to avoid the majority of pitting formation on these surfaces.

In terms of Vickers microhardness, mechanical polishing resulted on 206.0±1.1 $HV_{0.1}$, whereas this property was 194.4±4.6 $HV_{0.1}$ for the electrolytic polished sample, which confirms the strain-hardened layer in the first one.

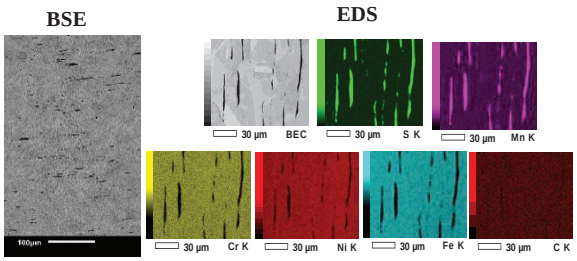


Fig. 2. SEM micrograph - backscattered electron image and EDS composition map of AISI 303 steel. The same microstructure was found for different surface finishing.

Table 1. AISI 303 specimens surface topography parameters before scratch tests.

| Parameter | Description | Mechanical Polishing | Electrolytic Polishing |
|---|---|---|---|
| $S_a$ (µm) | Arithmetic Mean Height | 0.014±0.001 | 0.117±0.042 |
| $S_q$ (µm) | Root Mean Square Height | 0.021±0.001 | 0.187±0.051 |
| $S_{sk}$ | Skewness | 0.196±0.282 | 0.996±0.452 |
| $S_{ku}$ | Kurtosis | 8.12 ±0.85 | 14.7±3.5 |
| $S_{dq}$ | Root Mean Square Gradient (Surface Slope) | 0.0174±0.0008 | 0.156±0.002 |
| $S_{pc}$ | Arithmetic Mean Peak Curvature ($\mu m^{-1}$) | 0.080±0.003 | 1.02±1.43 |

### *3.2. Vickers hardness and strain-hardened layer formation*

AISI 304 specimens mechanically polished were submitted to the Vickers microhardness tests, aiming to verify the effect of the strain-hardened layer. One-way ANOVA indicated that the average results from 50 to 2,000 gf are different. However, the T-test for comparison of two microhardness averages, following the methodology described by Box, Hunter and Hunter [15], was applied to the 50 and 100 gf, which are statically equal as well as the second group between 500 and 2.000 gf. Therefore, there is a transition between the both groups, and the hardness results for the first one were higher than the second one. From the data obtained with 100 gf, it is possible to obtain an indirect measurement of the thickness of the strain-hardened layer, applying Eq. (2) for the Vickers indenter [14]:

$$h = \frac{d}{2\sqrt{2}.\tan\left(\frac{\theta}{2}\right)} \quad (2)$$

In Eq. (2), h is the penetration depth; d is the diagonal average and θ is the internal angle of Vickers indenter (136°).

The calculated value for the thickness of the strain-hardened layer was 4.60±0.15 µm.

### *3.3. Apparent Coefficient of Friction*

The apparent coefficient of friction (COF) was calculated by the ratio between tangential force and normal force [20]. Average values of COF are plotted in Figure 3 as a function of normal load.

Literature results [11] allow predicting that the transition from ploughing to cutting occurs at 10 mN (Figure 1). In this reference [11], the authors developed experimental tests with several materials, including AISI 304 steel. Figure 3 indicates this transition has occurred from 50 to 60 mN for the AISI 303 steel electropolished specimen (EP) and from 40 to 50 mN in the AISI 303 steel mechanically polished specimen (MP). The cutting has prevailed at 60 mN for EP and 50 mN for MP. As shown in Figure 4, SEM micrographs confirmed the predominance of ploughing for 50 mN in EP and 40 mN in MP. The cutting has started prevailing at 60 mN for EP and 50 mN for MP.

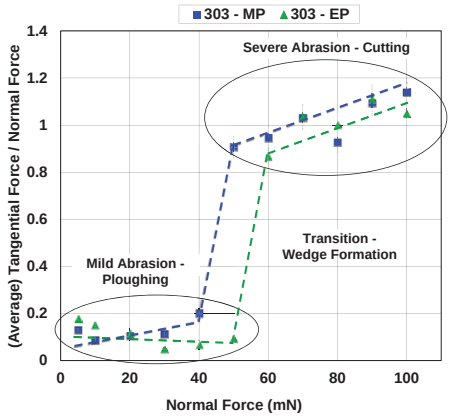


Fig. 3. Apparent Coefficient of Friction as a function of normal force in the mechanical polishing (MP) and electrolytic polishing (EP) of the AISI 303 steel specimens.

Furthermore, the following microstructural aspects can be highlighted in the AISI 303 steel specimens (Figure 5):

- Mechanical polishing (**MP**) – **point 1** – and Electrolytic polishing (**EP**) – **point 1**: a decrease in COF is apparently associated to the presence of MnS inclusions;
- Mechanical polishing (**MP**) – **point 2**: the material failure, with material detachment due to the abrasive action, results in a COF decrease;
- Mechanical polishing (**MP**) – **point 3** – and Electrolytic polishing (**EP**) – **point 2**: the scratch width presents a reduction at a specific point and an increase in the COF is observed. This result can be related to the microstructural region. With further diamond tip movement, the scratch width reverts to its original size, resulting in a drop of the COF;
- Electrolytic polishing (**EP**) – **point 3**: the topography causes a contact loss between the abrasive and the material tested, providing a COF value close to zero in this region and the localized interruption of the scratch.

### *3.4. Numerical Results*

The numerical results in Figure 6 allowed confirming two main behaviors:

(i-) electropolished (EP) surfaces have a higher mass removal than mechanical polished (MP), which is justified by the presence of the strain-hardened layer;

(ii-) MnS inclusions, with different morphologies, played a role as stress concentrators, providing a higher mass loss. This fact supports the better machinability of AISI 303 stainless steel (heterogeneous) compared with the homogeneous one. Figure 6 shows the chips formed during the abrasive process, which are consistent with the values of the mass removed considering the different normal forces. These results are in accordance with the literature related to manufacturing processes with tools with non-defined geometries [18–20].

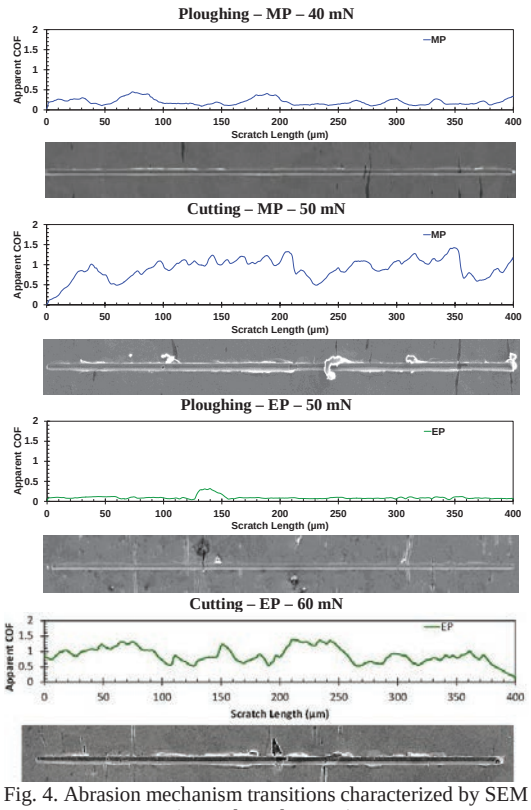


Fig. 4. Abrasion mechanism transitions characterized by SEM (secondary electrons).

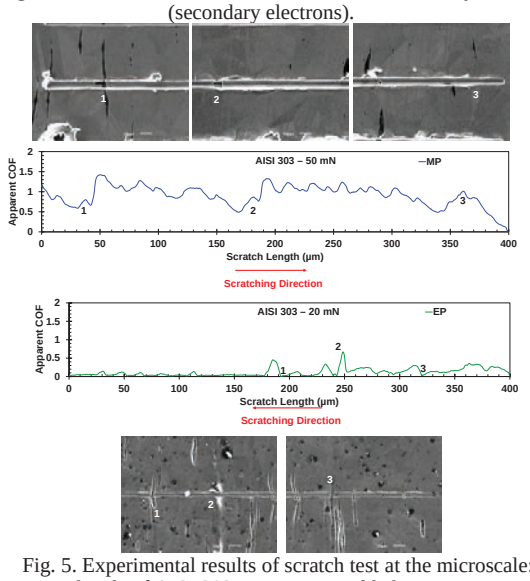


Fig. 5. Experimental results of scratch test at the microscale: details of AISI 303 microstructural behavior.

## 4. Conclusions and Final Remarks

The abrasion mechanisms in AISI 303 austenitic stainless steel specimens were evaluated by means of scratch tests at the micro-scale. Analysis was based on the apparent coefficient of friction and surface characterization: from 5 to 40 mN, micro-ploughing and wedge formation occurred; and from 50 to 100 mN, microcutting was observed. The experimental results are in disagreement with the map by Hokkirigawa, Kato and Li [11], which does not take into account the effect of the second phase particles, grain boundaries generated by different surface finishing; and/or the influence of strain-hardened layer. The numerical results confirmed that the manganese sulfide has improved the cutting process. The strain-hardened surface increased the material strength, which resulted on less mass removed during the scratch test. Based on simplified assumptions, this work is a preliminary study on how the surface integrity can affect the properties and features of the material surface, which presents high work hardening. Further numerical model by FEM, with higher complexity, can be developed based on the results and validations reported here.

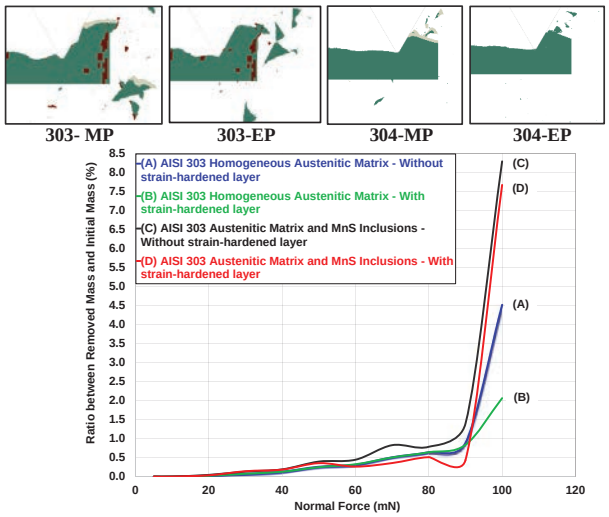


Fig. 6. Numerical results of mass removal by abrasion, obtained considering difference in surface finishing and microstructure.

### Acknowledgements

The authors would like to acknowledge to the financial support from the Brazilian research agencies - CNPq and FAPESP.

### References

[1] Peckner D, Bernstein IM. Handbook of stainless steels. McGraw-Hill New York, NY; 1977.
[2] British Stainless Steel Association (Collin Honess). Importance of Surface Finish in the Design of Stainless Steels [Internet]. 2015.Available from: http://www.bssa.org.uk/cms/File/surfacefinishbssaVer2.pdf
[3] Murr LE, Staudhammer KP, Hecker SS. Effects of strain state and strain rate on deformation-induced transformation in 304 stainless steel: Part II. Microstructural study. Metall Trans A. Springer; 1982;13(4):627–35.
[4] Nomani J, Pramanik A, Hilditch T, Littlefair G. Machinability study of first generation duplex (2205), second generation duplex (2507) and austenite stainless steel during drilling process. Wear. 2013;304(1–2):20–8.
[5] O'Sullivan D, Cotterell M. Machinability of austenitic stainless steel SS303. J Mater Process Technol. Elsevier; 2002;124(1):153–9.
[6] Lo KH, Shek CH, Lai JKL. Recent developments in stainless steels. Mater Sci Eng R Reports. 2009;65(4–6):39–104.
[7] Wang H, Jeong Y, Clausen B, Liu Y, McCabe RJ, Barlat F, et al. Effect of martensitic phase transformation on the behavior of 304 austenitic stainless steel under tension. Mater Sci Eng A. 2016;649:174–83.
[8] Kim YH, Kim KY, Lee YD. Nitrogen-Alloyed, Metastable Austenitic Stainless Steel for Automotive Structural Applications. Mater Manuf Process. 2004;19(1):51–9.
[9] Lee W-S, Lin C-F. Impact properties and microstructure evolution of 304L stainless steel. Mater Sci Eng A. 2001;308(1–2):124–35.
[10] Avery HS. Work hardening in relation to abrasion resistance. Climax Molybdenum Comp. Materials for the Mining Industry; 1974;43–77.
[11] Hokkirigawa K, Kato K, Li ZZ. The effect of hardness on the transition of the abrasive wear mechanism of steels. Wear. Elsevier; 1988;123(2):241–51.
[12] Souza L. Evaluation of cutting parameters and heat treatments in the turning process of three austenitic stainless steels. University of Sao Paulo; 2006. (in portuguese)
[13] Handbook ASM. Metallography and microstructures. 2nd Ed. Edited by GF Vander Voort, ASM Intenational. 2004.
[14] Yovanovich MM. Micro and macro hardness measurements, correlations, and contact models. Collection of technical papers—44th AIAA aerospace sciences meeting. 2006. p. 11702–29.
[15] Box GEP, Hunter JS, Hunter WG. Statistics for experimenters: design, innovation, and discovery. 2nd Ed. AMC. 2005.
[16] Krasauskas P, Kilikevičius S, Česnavičius R, Pačenga D. Experimental analysis and numerical simulation of the stainless AISI 304 steel friction drilling process. Mechanika. 2015;20(6):590–5.
[17] Chagas GMP, Machado IF. Numerical Model of Machining Considering the Effect of MnS Inclusions in an Austenitic Stainless Steel. Procedia CIRP. Elsevier; 2015;31:533–8.
[18] Dzugan J, Spaniel M, Konopík P, Ruzicka J, Kuzelka J. Identification of Ductile Damage Parameters for Austenitic Steel. World Acad Sci Eng Technol. 2012;6(5):1291–6.
[19] Bhuyan A, Gregory B, Lei H, Yee SY, Gianchandani YB. Pulse and DC electropolishing of stainless steel for stents and other devices. Sensors, 2005 IEEE. 2005. p. 314–7.
[20] Wredenberg F, Larsson P-L. On the numerics and correlation of scratch testing. J Mech Mater Struct. Mathematical Sciences Publishers; 2007;2(3):573–94.